ISSN 2176-5480

22nd International Congress of Mechanical Engineering (COBEM 2013)
November 3-7, 2013, Ribeirão Preto, SP, Brazil

DYNAMIC MODELING OF CABLES WITH UNDERWATER APPLICATIONS

Adriana Elisa Ladeira Pereira
Sebastião Cícero Pinheiro Gomes
Universidade Federal do Rio Grande, Av. Itália, km8, 96201-900, Rio Grande, RS
e-mails:sebastiaogomes@furg.br; aelpereira@furg.br

Alvaro Luiz de Bortoli
Universidade Federal do Rio Grande do Sul, Av. Bento Gonçalves, P. O. Box 15080, Porto Alegre, RS
e-mail: dbortoli@ufrgs.br

Abstract. *This paper presents a study on a new modeling formalism of flexible structures cable used in underwater applications. Forces arising from the interaction between the fluid (water) and structure were modeled as proportional to the square of the relative velocity. An immediate application could be in umbilicals underwater vehicles type ROV (remotely operated vehicle). The primary basis for the formulation is to assume that the continuous flexibility is represented by a discrete approach, consisting of rigid links connected by elastic joints, allowing movement in three dimensions. Each elastic joint allows three independent movements, called elevation, azimuth and torsion (twist). A significant contribution of the proposed formalism is the development of a compact equation that allows obtaining the Lagrangian of the system directly and automatically, regardless of the number of links chosen to form a chain of rigid bodies connected by flexible joints to represent the continuous flexibility of the cable.*

Keywords: *Modeling, cables, underwater, ROV*

1. INTRODUCTION

The dynamic modeling of cables had difficulties due to the natural complexity of the physical problem, especially when working in fact considering the cable spatial movement. Because of this, some articles have proposed simplified approximations to the dynamics of the cable, considering, for example, that the movement is restricted to a single plane [15]. In this article it is used the formulation proposed in Pereira *et. al.,* [17] for dynamic modeling of a cable and a greater emphasis to the solution is presented. It is further considered that the cable is underwater and the considered drag is proportional to the square of the relative velocity between the fluid and the cable.

Most of the literature on the subject deals with modeling of underwater cables using the finite element technique. WANG et. al. [1] used the Finite Element Method and investigated the vibrations of an underwater cable with a load at its end point. Gosling and Korban [2] described a finite element formulation for structural analysis of cables considering its flexibility finite and continuous. ROCHINHA et. al. [3] presented a numerical model for umbilical hyper-elastic cables with large displacements and rotations and solved the problem using equations discretized by the Finite Element Method. Other authors also used the finite element method for the structural dynamic analysis of flexible cables ([4], [5], [6], [7]). Some authors have developed their works with the implementation of a static analysis of a cable ([8], [9], [10], [11]), using the method of finite differences. Zhu et. al. [12] proposed a discrete model to determine the forces that an umbilical cable exerts on a ROV and showed numerical results. Raman-Nair et. al. [13] have used a discrete model to reproduce structural forces acting into a flexible marine riser under effects of flow and pressure of fluid within the riser. In [14] is presented a kinematic model for parallel mechanisms and also made analysis of singularities for special cases of parallel mechanisms. In [15] a simulation of the dynamics of a cable for kities is made considering each link with one degree of freedom mass spring damper model. The simulation is performed using MSC ADAMS software and the cable is considered moving in a plane.

In this paper it is used a new formalism, which can be considered as an expansion pack of the modeling formalism proposed in Gomes *et. al.* [16], for a manipulator with a flexible link (in this case, the flexibility of the link is planar and each joint has a single degree of freedom). However, in the case of cable dynamic, the flexible joints have three degrees of freedom (azimuth, elevation and twist) and the flexibilty takes place in space. One main advantage of the proposed formalism is that dynamic variables of the model are physically measurable (angular positions and velocities) and thus, simulations can be performed and compared with experiments. Another advantage of this formalism is the compact single formula obtained for the Lagrangian of the system, regardless the number of degrees of freedom of the dynamic model. Dynamic model is obtaining as a function of physical variables such as positions and angular velocities, and this allows greater ease in interacting with other dynamics, such as a ROV at the free end of the cable, for example. The formalism also allows the inclusion of external dynamics to the model, such as those arising from currents, in the case of underwater cables.

2. THEORETICAL ELEMENTS

Consider a cable as shown in Fig. 1, fixed at its top to a base and free at its bottom, where there is a mass m_c. The main idea of the method is to divide the cable into small rigid elements (links l_i in black as shown in Fig. 1) connected by flexible joints that allow three independent free movements, entitled here as azimuth, elevation and twist, and relative to the previous link in the articulated chain. It should be noted that another motion could be considered: linear extension that has been neglected in this article. Each joint has a fictitious elastic nature and therefore three elastic constants with their respective damping are parameters that define the physical nature of the joint. In summary, the proposal introduces a method to determine the Lagrangian of the system in an algorithmic form, regardless of the number of elements chosen to divide the flexible structure. The application of the Euler-Lagrange equation to all degrees of freedom of the system allows obtaining the final dynamic model.

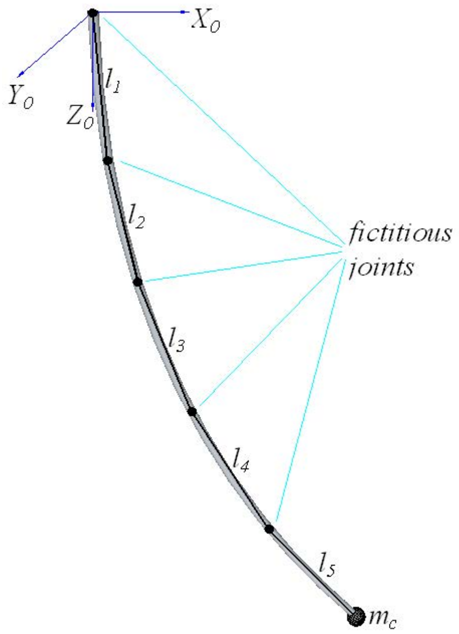

Fig. 1. Flexible structure and its discrete representation.

At each link the mass is lumped ($m_1, m_2, m_3 \ldots m_n$) at its center of mass (x_1, y_1, z_1), (x_2, y_2, z_2),..., (x_n, y_n, z_n) and (x_c, y_c, z_c) are the coordinates of the center of mass of the load m_c. In each fictitious joint the angles of azimuth, elevation and twist are considered: θ_{ia} is the azimuth angle, θ_{ie} the elevation angle and θ_{iT} the angle of twist, as shown in Fig. 3; *i* varies from 1 to the number of fictitious joints (*n*).

The system $X_i Y_i Z_i$ has $O_i Z_i$ as the axis parallel to the OZ_0 axis of the initial reference system (always in the vertical direction); the $O_i Y_i$ is parallel to the projection of the previous rigid link (projection in the horizontal plane). In the example shown in Fig. 3, the projection of the link l_1 in the horizontal plane has the same direction as the line *r* and the Y_1 axis is placed parallel to the line *r*. The axis $O_i X_i$ is orthogonal to the axis $O_i Y_i$. Three elastic constants are considered at each joint, ie, in the *i-th* joint there is the elastic constants k_{ia} , k_{ie} , k_{iT} , due to the angles of azimuth, elevation and twist, respectively.

It is important to remark that due to the convention adopted, the elevation angles are symmetrical with respect to the Z_{i-1} axis in each α_i plane, as illustrated in Fig. 2 (left) and the azimuth angle θ_{ia} is always the smallest angle between the axis Y_{i-1} and the plane α_i. Another convention adopted is related to the base inertial frame ($X_0 Y_0 Z_0$). Consider an inertial geodetic system $X_G Y_G Z_G$, as seen in Fig. 2 (right), with the Z_G axis pointing to the center of the Earth and Y_G to the South Pole. The inertial system $X_0 Y_0 Z_0$ is placed such that Z_0 points to the center of the Earth and Y_0 in the same direction of the horizontal projection of the link 1 at the beginning of the first movement of the cable.

If the movement of the cable is caused by a known external perturbation (ocean current with known direction, for example) it is easy to find the angle between Y_G and Y_0 . The azimuth angles of the links are then taken with respect to the axes Y_i (i=0,1,…,n-1) and whenever there exist deformations of the cable, which cause movements, the cable geometric configuration can no longer be contained within a single plane. This means that if the cable is with elevation, azimuth and twist angles different from zero, all angles will tend to zero (in the absence of external torques) due to gravity and the internal elastic torques.
The kinetic energy is defined by:

$$E_C = E_{C_R} + E_{C_T} \tag{1}$$

where E_{C_R} is the kinetic energy due to rotation and E_{C_T} is the kinetic energy due to the translation movements. Considering that I_{R_1} , I_{R_2} , I_{R_3} , …, I_{R_n} are the rotation moments of inertia of the rigid links and I_{T_1} , I_{T_2} , I_{T_3} , …, I_{T_n} , I_{T_c} are the twist moments of inertia, E_{C_R} and E_{C_T} may be written as follows:

$$\begin{aligned} E_{C_R} = {} & \frac{1}{2} I_{R_1} \dot{\theta}_{1e}^2 + \frac{1}{2} I_{R_2} \left(\dot{\theta}_{1e} + \dot{\theta}_{2e}\right)^2 + \frac{1}{2} I_{R_3} \left(\dot{\theta}_{1e} + \dot{\theta}_{2e} + \dot{\theta}_{3e}\right)^2 + \ldots + \frac{1}{2} I_{R_n} \left(\sum_{i=1}^{n} \dot{\theta}_{ie}\right)^2 + \\ & + \frac{1}{2} I_{T_1} \dot{\theta}_{1\mathrm{T}}^2 + \frac{1}{2} I_{T_2} \left(\dot{\theta}_{1T} + \dot{\theta}_{2\mathrm{T}}\right) + \frac{1}{2} I_{T_3} \left(\dot{\theta}_{1T} + \dot{\theta}_{2\mathrm{T}} + \dot{\theta}_{3\mathrm{T}}\right)^3 + \ldots + \frac{1}{2} \left(I_{T_n} + I_{T_c}\right) \left(\sum_{i=1}^{n} \dot{\theta}_{iT}\right)^2 \end{aligned} \tag{2}$$

$$\begin{aligned} E_{C_T} = {} & \frac{1}{2} m_1 \left(\dot{x}_1^2 + \dot{y}_1^2 + \dot{z}_1^2\right) + \frac{1}{2} m_2 \left(\dot{x}_2^2 + \dot{y}_2^2 + \dot{z}_2^2\right) + \frac{1}{2} m_3 \left(\dot{x}_3^2 + \dot{y}_3^2 + \dot{z}_3^2\right) + \ldots + \\ & + \frac{1}{2} m_n \left(\dot{x}_n^2 + \dot{y}_n^2 + \dot{z}_n^2\right) + \frac{1}{2} m_c \left(\dot{x}_c^2 + \dot{y}_c^2 + \dot{z}_c^2\right) \end{aligned} \tag{3}$$

As each link has a cylindrical shape, I_{Ri} is the moment of inertia about an axis perpendicular to link i passing through its center of mass, ie $I_{Ri} = (1/12) m_i l_i^2$, and m_i and l_i are the mass and the length of link i. I_{T_i} is the moment of inertia about a longitudinal axis of the link, and passing through its center of mass, ie $I_{T_\mathrm{i}} = (1/2) m_i r_i^2$, and r_i is the radius of the link i. It is important to point out that it was neglected the kinetic energy due to rotational movement of azimuth and still considered, by approximation, that the elevation movements of the links take place in a plan (only for the calculation of the rotational kinetic energy due to elevation). The twisting motion is also considered as the cable was stretched, by approximation. As the rotational kinetic energy is less significant than the translation, these considerations do not compromise the quality of the model and significantly simplify the development of its differential equations. In summary, the emphasis is on translational kinetic energy and then the classical Euler-Lagrange formalism to obtain the dynamic model is used.

The potential energy is defined by:

$$\begin{aligned} E_p = {} & \frac{1}{2} k_{1e} \theta_{1e}^2 + \frac{1}{2} k_{2e} \left(\theta_{2e} - \theta_{1e}\right)^2 + \frac{1}{2} k_{3e} \left(\theta_{3e} - \theta_{2e}\right)^2 + \ldots + \frac{1}{2} k_{ne} \left(\theta_{ne} - \theta_{(n-1)e}\right)^2 + \\ & + \frac{1}{2} k_{1a} \theta_{1a}^2 + \frac{1}{2} k_{2a} \left(\theta_{2a} - \theta_{1a}\right)^2 + \frac{1}{2} k_{3a} \left(\theta_{3a} - \theta_{2a}\right)^2 + \ldots + \frac{1}{2} k_{na} \left(\theta_{na} - \theta_{(n-1)a}\right)^2 + \\ & + \frac{1}{2} k_{1\mathrm{T}} \theta_{1\mathrm{T}}^2 + \frac{1}{2} k_{2\mathrm{T}} \left(\theta_{2\mathrm{T}} - \theta_{1\mathrm{T}}\right)^2 + \frac{1}{2} k_{3\mathrm{T}} \left(\theta_{3\mathrm{T}} - \theta_{2\mathrm{T}}\right)^2 + \ldots + \frac{1}{2} k_{nT} \left(\theta_{nT} - \theta_{(n-1)T}\right)^2 \\ & + m_1\, g\, h_1 + m_2\, g\, h_2 + m_3\, g\, h_3 + \ldots + m_n g h_n \end{aligned} \tag{4}$$

where k_{ie}, k_{ia} and k_{it} correspond to the elastic constants for movements of elevation, azimuth and twist, respectively, with i = 1, ..., n, where n is the number of fictitious joints, and the heights h_i used in gravitational potential energy are defined as follows:

$$h_1 = \frac{l_1}{2}\left(1-\cos\theta_{1e}\right),\, h_2 = l_1\left(1-\cos\theta_{1e}\right)+\frac{l_2}{2}\left(1-\cos\theta_{2e}\right),\ldots, h_n = \sum_{i=1}^{n-1} l_i\left(1-\cos\theta_{ie}\right)+\frac{l_n}{2}\left(1-\cos\theta_{ne}\right) \tag{5}$$

From the Eqs. (2), (3) and (4), the Lagrangian of the system can be written as:

$$\begin{aligned} L = {} & \frac{1}{2}I_{R_1}\dot{\theta}_{1e}^2 + \frac{1}{2}I_{R_2}\left(\dot{\theta}_{1e}+\dot{\theta}_{2e}\right)^2 + \frac{1}{2}I_{R_3}\left(\dot{\theta}_{1e}+\dot{\theta}_{2e}+\dot{\theta}_{3e}\right)^2 + \ldots + \frac{1}{2}I_{R_n}\left(\sum_{i=1}^{n}\dot{\theta}_{ie}\right)^2 + \\ & + \frac{1}{2}I_{T_1}\dot{\theta}_{1\mathrm{T}}^2 + \frac{1}{2}I_{T_2}\left(\dot{\theta}_{1T}+\dot{\theta}_{2\mathrm{T}}\right) + \frac{1}{2}I_{T_3}\left(\dot{\theta}_{1T}+\dot{\theta}_{2\mathrm{T}}+\dot{\theta}_{3\mathrm{T}}\right)^3 + \ldots + \frac{1}{2}\left(I_{T_n}+I_{T_c}\right)\left(\sum_{i=1}^{n}\dot{\theta}_{iT}\right)^2 + \\ & + \frac{1}{2}m_1\left(\dot{x}_1^2+\dot{y}_1^2+\dot{z}_1^2\right) + \frac{1}{2}m_2\left(\dot{x}_2^2+\dot{y}_2^2+\dot{z}_2^2\right) + \frac{1}{2}m_3\left(\dot{x}_3^2+\dot{y}_3^2+\dot{z}_3^2\right) + \ldots \\ & + \frac{1}{2}m_n\left(\dot{x}_n^2+\dot{y}_n^2+\dot{z}_n^2\right) + \frac{1}{2}m_c\left(\dot{x}_c^2+\dot{y}_c^2+\dot{z}_c^2\right) - \frac{1}{2}k_{1e}\theta_{1e}^2 - \frac{1}{2}k_{2e}\left(\theta_{2e}-\theta_{1e}\right)^2 + \\ & - \frac{1}{2}k_{3e}\left(\theta_{3e}-\theta_{2e}\right)^2 - \ldots - \frac{1}{2}k_{ne}\left(\theta_{ne}-\theta_{(n-1)e}\right)^2 - \frac{1}{2}k_{1a}\theta_{1a}^2 - \frac{1}{2}k_{2a}\left(\theta_{2a}-\theta_{1a}\right)^2 + \\ & - \frac{1}{2}k_{3a}\left(\theta_{3a}-\theta_{2a}\right)^2 - \ldots - \frac{1}{2}k_{na}\left(\theta_{na}-\theta_{(n-1)a}\right)^2 - \frac{1}{2}k_{1\mathrm{T}}\theta_{1\mathrm{T}}^2 - \frac{1}{2}k_{2\mathrm{T}}\left(\theta_{2\mathrm{T}}-\theta_{1\mathrm{T}}\right)^2 + \\ & - \frac{1}{2}k_{3\mathrm{T}}\left(\theta_{3\mathrm{T}}-\theta_{2\mathrm{T}}\right)^2 - \ldots - \frac{1}{2}k_{nT}\left(\theta_{nT}-\theta_{(n-1)T}\right)^2 - m_1\, g\, h_1 - m_2\, g\, h_2 - m_3\, g\, h_3 - \ldots - m_n g h_n \end{aligned} \tag{6}$$

From the Eqs. (5) and (6) and considering that $\theta_{0e}=\theta_{0a}=\theta_{0T}=0$ and $h_0=0$, results

$$\begin{aligned} L = \sum_{\ell=1}^{n} \Bigg\{ & \frac{1}{2}I_{R_\ell}\left(\sum_{i=1}^{\ell}\dot{\theta}_{ie}\right)^2 + \frac{1}{2}I_{T_\ell}\left(\sum_{i=1}^{\ell}\dot{\theta}_{iT}\right)^2 + \frac{1}{2}m_\ell\left(\dot{x}_\ell^2+\dot{y}_\ell^2+\dot{z}_\ell^2\right) - \frac{1}{2}k_{\ell e}\left(\theta_{\ell e}-\theta_{(\ell-1)e}\right)^2 + \\ & - \frac{1}{2}k_{\ell a}\left(\theta_{\ell a}-\theta_{(\ell-1)a}\right)^2 - \frac{1}{2}k_{\ell T}\left(\theta_{\ell T}-\theta_{(\ell-1)T}\right)^2 - m_\ell g\left[\sum_{i=1}^{\ell-1} l_i\left(1-\cos\theta_{ie}\right)+\frac{l_\ell}{2}\left(1-\cos\theta_{\ell e}\right)\right]\Bigg\} + \\ & + \frac{1}{2}I_{T_c}\dot{\theta}_{nT}^2 + \frac{1}{2}m_c\left(\dot{x}_c^2+\dot{y}_c^2+\dot{z}_c^2\right) \end{aligned} \tag{7}$$

3. THE LAGRANGEAN IN ANGULAR COORDINATES

The Lagrangian equations depending only on the angular coordinates where obtained through the development of kinematic relations obtained from homogeneous transformations, as explained below. The first fictitious joint is placed at the origin of the reference system $X_0Y_0Z_0$, and the angles of azimuth θ_{1a} and elevation θ_{1e} are considered according to Figs. 3 and 4. Fig. 4 shows the first two reference systems, the links and the angles. From this figure it is concluded that the coordinates of the second fictitious joint in the $X_0Y_0Z_0$ reference system are:

$$\begin{cases} x_{0_1} = l_1 \sin\theta_{1e}\sin\theta_{1a} \\ y_{0_1} = l_1 \sin\theta_{1e}\cos\theta_{1a} \\ z_{0_1} = l_1 \cos\theta_{1e} \end{cases} \tag{8}$$

and the coordinates of the center of mass of the first link (l_1) are:

ISSN 2176-5480

$$\begin{cases} x_1 = \dfrac{l_1}{2}\sin\theta_{1e}\sin\theta_{1a} \\ y_1 = \dfrac{l_1}{2}\sin\theta_{1e}\cos\theta_{1a} \\ z_1 = \dfrac{l_1}{2}\cos\theta_{1e} \end{cases} \tag{9}$$

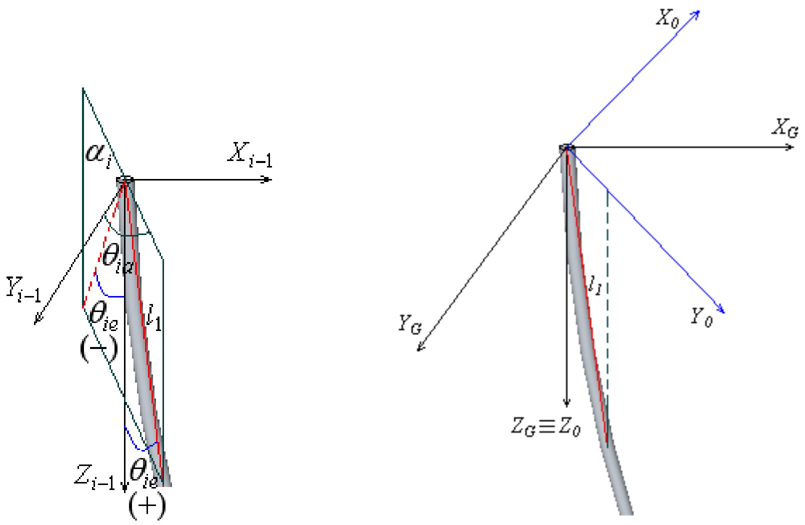

Fig. 2. Representation of the conventions.

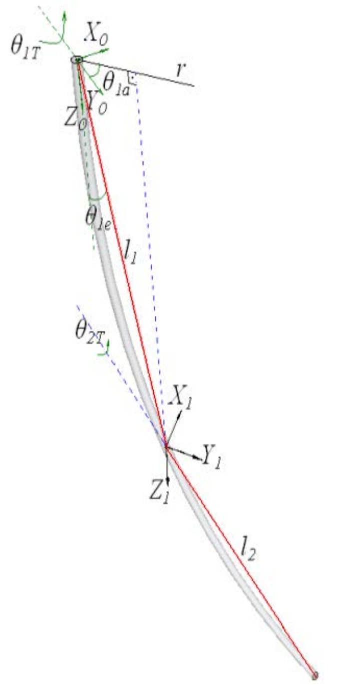

Fig. 3. Angles of azimuth, elevation and twist in the ith joint.

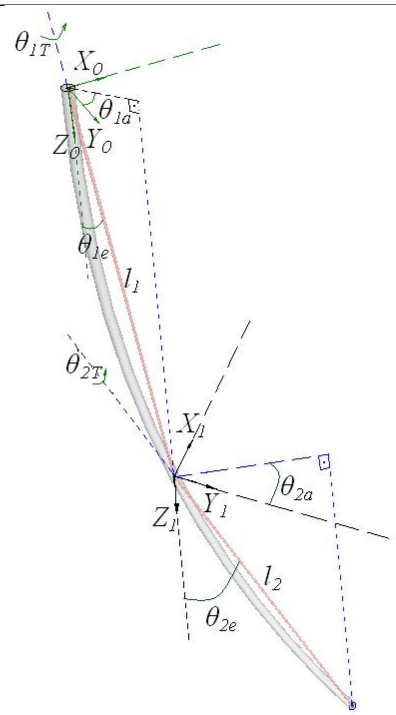

Fig. 4. Geometric representation of the first two reference systems.

A new reference system ($X_1Y_1Z_1$) is incorporated into the flexible structure, centered on the second fictitious joint, as illustrated in Fig. 3, according to the convention explained previously.

Considering Eqs. (8), it can be shown that the homogeneous transformation relating the systems $X_0Y_0Z_0$ and $X_1Y_1Z_1$ has the form:

$$H_{0_1} = \begin{bmatrix} \cos\theta_{1a} & \sin\theta_{1a} & 0 & l_1 \sin\theta_{1e} \sin\theta_{1a} \\ -\sin\theta_{1a} & \cos\theta_{1a} & 0 & l_1 \sin\theta_{1e} \cos\theta_{1a} \\ 0 & 0 & 1 & l_1 \cos\theta_{1e} \\ 0 & 0 & 0 & 1 \end{bmatrix} \tag{10}$$

Considering another link and placing the reference system $X_2Y_2Z_2$ at the third fictitious joint, the homogeneous transformation relating the systems $X_1Y_1Z_1$ and $X_2Y_2Z_2$ has the form:

$$H_{1_2} = \begin{bmatrix} \cos\theta_{2a} & \sin\theta_{2a} & 0 & l_2 \sin\theta_{2e} \sin\theta_{2a} \\ -\sin\theta_{2a} & \cos\theta_{2a} & 0 & l_2 \sin\theta_{2e} \cos\theta_{2a} \\ 0 & 0 & 1 & l_2 \cos\theta_{2e} \\ 0 & 0 & 0 & 1 \end{bmatrix} \tag{11}$$

Knowing that $H_{0_2} = H_{0_1} \cdot H_{1_2}$ it can be written:

$$H_{0_2} = \begin{bmatrix} \cos(\theta_{1a}+\theta_{2a}) & \sin(\theta_{1a}+\theta_{2a}) & 0 & l_2 \sin\theta_{2e} \sin(\theta_{1a}+\theta_{2a}) + l_1 \sin\theta_{1e} \sin\theta_{1a} \\ -\sin(\theta_{1a}+\theta_{2a}) & \cos(\theta_{1a}+\theta_{2a}) & 0 & l_2 \sin\theta_{2e} \cos(\theta_{1a}+\theta_{2a}) + l_1 \sin\theta_{1e} \cos\theta_{1a} \\ 0 & 0 & 1 & l_2 \cos\theta_{2e} + l_1 \cos\theta_{1e} \\ 0 & 0 & 0 & 1 \end{bmatrix} \tag{12}$$

Therefore, the coordinates of the center of mass of the second link (l_2) written in the inertial reference of the base ($X_0Y_0Z_0$) are:

$$\begin{cases} x_2 = \dfrac{l_2}{2} \sin\theta_{2e} \sin(\theta_{1a}+\theta_{2a}) + l_1 \sin\theta_{1e} \sin\theta_{1a} \\ y_2 = \dfrac{l_2}{2} \sin\theta_{2e} \cos(\theta_{1a}+\theta_{2a}) + l_1 \sin\theta_{1e} \cos\theta_{1a} \\ z_2 = \dfrac{l_2}{2} \cos\theta_{2e} + l_1 \cos\theta_{1e} \end{cases} \tag{13}$$

Adding one more link and proceeding in a similar way as explained previously, the coordinates of the center of mass of the third link wrote in the inertial reference of the base are:

$$\begin{cases} x_3 = \dfrac{l_3}{2} \sin\theta_{3e} \sin(\theta_{1a}+\theta_{2a}+\theta_{3a}) + l_2 \sin\theta_{2e} \sin(\theta_{1a}+\theta_{2a}) + l_1 \sin\theta_{1e} \sin\theta_{1a} \\ y_3 = \dfrac{l_3}{2} \sin\theta_{3e} \cos(\theta_{1a}+\theta_{2a}+\theta_{3a}) + l_2 \sin\theta_{2e} \cos(\theta_{1a}+\theta_{2a}) + l_1 \sin\theta_{1e} \cos\theta_{1a} \\ z_3 = \dfrac{l_3}{2} \cos\theta_{3e} + l_2 \cos\theta_{2e} + l_1 \cos\theta_{1e} \end{cases} \tag{14}$$

In a general way, Eqs. (9), (13) and (14) suggest an algorithm to write the coordinates of the center of mass of any link of the chain, in the form:

ISSN 2176-5480

$$\begin{cases} x_k = \dfrac{l_k}{2}\sin\theta_{ke}\sin\left(\sum_{i=1}^{k}\theta_{ia}\right) + \sum_{j=1}^{k-1}\left[l_j \sin\theta_{je}\sin\left(\sum_{i=1}^{j}\theta_{ia}\right)\right] \\ y_k = \dfrac{l_k}{2}\sin\theta_{ke}\cos\left(\sum_{i=1}^{k}\theta_{ia}\right) + \sum_{j=1}^{k-1}\left[l_j \sin\theta_{je}\cos\left(\sum_{i=1}^{j}\theta_{ia}\right)\right] \\ z_k = \dfrac{l_k}{2}\cos\theta_{ke} + \sum_{j=1}^{k-1} l_j \cos\theta_{je} \end{cases} \tag{15}$$

$$\begin{cases} x_c = \sum_{j=1}^{n}\left[l_j \sin\theta_{je}\sin\left(\sum_{i=1}^{j}\theta_{ia}\right)\right] \\ y_c = \sum_{j=1}^{n}\left[l_j \sin\theta_{je}\cos\left(\sum_{i=1}^{j}\theta_{ia}\right)\right] \\ z_c = \sum_{j=1}^{n} l_j \cos\theta_{je} \end{cases} \tag{16}$$

The time derivatives of the Eqs. (15) and (16) are obtained in the forms:

$$\begin{cases} \dot{x}_k = \dfrac{l_k}{2}\left[\sin\theta_{ke}\cos\left(\sum_{i=1}^{k}\theta_{ia}\right)\sum_{i=1}^{k}\dot{\theta}_{ia} + \cos\theta_{ke}\sin\left(\sum_{i=1}^{k}\theta_{ia}\right)\dot{\theta}_{ke}\right] + \\ \qquad + \sum_{j=1}^{k-1} l_j\left[\sin\theta_{je}\cos\left(\sum_{i=1}^{j}\theta_{ia}\right)\sum_{i=1}^{j}\dot{\theta}_{ia} + \cos\theta_{je}\sin\left(\sum_{i=1}^{j}\theta_{ia}\right)\dot{\theta}_{je}\right] \\ \dot{y}_k = \dfrac{l_k}{2}\left[-\sin\theta_{ke}\sin\left(\sum_{i=1}^{k}\theta_{ia}\right)\sum_{i=1}^{k}\dot{\theta}_{ia} + \cos\theta_{ke}\cos\left(\sum_{i=1}^{k}\theta_{ia}\right)\dot{\theta}_{ke}\right] + \\ \qquad + \sum_{j=1}^{k-1} l_j\left[-\sin\theta_{je}\sin\left(\sum_{i=1}^{j}\theta_{ia}\right)\sum_{i=1}^{j}\dot{\theta}_{ia} + \cos\theta_{je}\cos\left(\sum_{i=1}^{j}\theta_{ia}\right)\dot{\theta}_{je}\right] \\ \dot{z}_k = -\dfrac{l_k}{2}\sin\theta_{ke}\dot{\theta}_{ke} - \sum_{j=1}^{k-1} l_j \sin\theta_{je}\dot{\theta}_{je} \end{cases} \tag{17}$$

$$\begin{cases} \dot{x}_c = \sum_{j=1}^{n} l_j\left[\sin\theta_{je}\cos\left(\sum_{i=1}^{j}\theta_{ia}\right)\sum_{i=1}^{j}\dot{\theta}_{ia} + \cos\theta_{je}\sin\left(\sum_{i=1}^{j}\theta_{ia}\right)\dot{\theta}_{je}\right] \\ \dot{y}_c = \sum_{j=1}^{n} l_j\left[-\sin\theta_{je}\sin\left(\sum_{i=1}^{j}\theta_{ia}\right)\sum_{i=1}^{j}\dot{\theta}_{ia} + \cos\theta_{je}\cos\left(\sum_{i=1}^{j}\theta_{ia}\right)\dot{\theta}_{je}\right] \\ \dot{z}_c = -\sum_{j=1}^{n} l_j \sin\theta_{je}\dot{\theta}_{je} \end{cases} \tag{18}$$

Using Eq. (7) and again considering $\theta_{0e} = \theta_{0a} = \theta_{0T} = 0$ and $h_0 = 0$ the Lagrangian of the system can be obtained to the most general case of the $3n$ degrees of freedom and entirely written in terms of angular coordinates:

$$
\begin{aligned}
L = \sum_{\ell=1}^{n} \Bigg\{ & \frac{1}{2} I_{R_\ell} \left(\sum_{i=1}^{\ell} \dot{\theta}_{ie} \right)^2 + \frac{1}{2} I_{T_\ell} \left(\sum_{i=1}^{\ell} \dot{\theta}_{iT} \right)^2 - \frac{1}{2} k_{\ell e} \left(\theta_{\ell e} - \theta_{(\ell-1)e} \right)^2 - \frac{1}{2} k_{\ell a} \left(\theta_{\ell a} - \theta_{(\ell-1)a} \right)^2 + \\
& - \frac{1}{2} k_{\ell T} \left(\theta_{\ell T} - \theta_{(\ell-1)T} \right)^2 - m_\ell g \left[\sum_{i=1}^{\ell-1} l_i \left(1 - \cos\theta_{ie} \right) + \frac{l_\ell}{2} \left(1 - \cos\theta_{\ell e} \right) \right] \Bigg\} + \\
& + \sum_{\ell=1}^{n} \frac{m_\ell}{2} \Bigg\{ \frac{l_\ell}{2} \left[\sin\theta_{\ell e} \cos\left(\sum_{i=1}^{\ell} \theta_{ia} \right) \sum_{i=1}^{\ell} \dot{\theta}_{ia} + \cos\theta_{\ell e} \sin\left(\sum_{i=1}^{\ell} \theta_{ia} \right) \dot{\theta}_{\ell e} \right] + \\
& + \sum_{j=1}^{\ell-1} l_j \left[\sin\theta_{je} \cos\left(\sum_{i=1}^{j} \theta_{ia} \right) \sum_{i=1}^{j} \dot{\theta}_{ia} + \cos\theta_{je} \sin\left(\sum_{i=1}^{j} \theta_{ia} \right) \dot{\theta}_{je} \right] \Bigg\}^2 + \\
& + \sum_{\ell=1}^{n} \frac{m_\ell}{2} \Bigg\{ \frac{l_\ell}{2} \left[- \sin\theta_{\ell e} \sin\left(\sum_{i=1}^{\ell} \theta_{ia} \right) \sum_{i=1}^{\ell} \dot{\theta}_{ia} + \cos\theta_{\ell e} \cos\left(\sum_{i=1}^{\ell} \theta_{ia} \right) \dot{\theta}_{\ell e} \right] + \\
& + \sum_{j=1}^{\ell-1} l_j \left[- \sin\theta_{je} \sin\left(\sum_{i=1}^{j} \theta_{ia} \right) \sum_{i=1}^{j} \dot{\theta}_{ia} + \cos\theta_{je} \cos\left(\sum_{i=1}^{j} \theta_{ia} \right) \dot{\theta}_{je} \right] \Bigg\}^2 + \\
& + \sum_{\ell=1}^{n} \frac{m_\ell}{2} \left[- \frac{l_\ell}{2} \sin\theta_{\ell e} \dot{\theta}_{\ell e} - \sum_{j=1}^{\ell-1} l_j \sin\theta_{je} \dot{\theta}_{je} \right]^2 + \frac{1}{2} I_{T_c} \dot{\theta}_{nT}^2 + \\
& + \frac{1}{2} m_c \left\{ \sum_{\ell=1}^{n} l_\ell \left[\sin\theta_{\ell e} \cos\left(\sum_{i=1}^{\ell} \theta_{ia} \right) \sum_{i=1}^{\ell} \dot{\theta}_{ia} + \cos\theta_{\ell e} \sin\left(\sum_{i=1}^{\ell} \theta_{ia} \right) \dot{\theta}_{\ell e} \right] \right\}^2 + \\
& + \frac{1}{2} m_c \left\{ \sum_{\ell=1}^{n} l_\ell \left[- \sin\theta_{\ell e} \sin\left(\sum_{i=1}^{\ell} \theta_{ia} \right) \sum_{i=1}^{\ell} \dot{\theta}_{ia} + \cos\theta_{\ell e} \cos\left(\sum_{i=1}^{\ell} \theta_{ia} \right) \dot{\theta}_{\ell e} \right] \right\}^2 + \\
& + \frac{1}{2} m_c \left[- \sum_{\ell=1}^{n} l_\ell \sin\theta_{\ell e} \dot{\theta}_{\ell e} \right]^2
\end{aligned}
\tag{19}
$$

4. DYNAMIC MODEL

After knowing the Lagrangian of the system, it becomes easy to obtain its dynamic model using the Euler-Lagrange equation, applied to each one of the $3n$ degrees of freedom. The dynamic model equation is written in the form:

$$
I\left(\vec{\theta}\right)\ddot{\vec{\theta}} + C\,\dot{\vec{\theta}} + K\vec{\theta} + \vec{f}\left(\vec{\theta},\dot{\vec{\theta}}\right) = \vec{T}_m \tag{20}
$$

where $\vec{\theta} = \left[\theta_{1e} \quad \theta_{2e} \quad \theta_{3e} \quad \theta_{1a} \quad \theta_{2a} \quad \theta_{3a} \quad \theta_{1\mathrm{T}} \quad \theta_{2\mathrm{T}} \quad \theta_{3\mathrm{T}}\right]^T$ (for the case of three fictitious joints). $I\left(\vec{\theta}\right)$ is the inertia matrix, C is the friction coefficient matrix, K is the matrix elastic constants and $\vec{f}\left(\vec{\theta},\dot{\vec{\theta}}\right)$is the Coriolis-Centrifuges torques. If the cable is submerged, the vector with the external torques has the form:

$$
\vec{T}_m = \vec{\tau}_m + \vec{\tau}_a + \vec{\tau}_e \tag{21}
$$

where $\vec{\tau}_m$ is the external torque applied, for example, by a ROV attached to the free end of the cable (or an ocean current, for example), $\vec{\tau}_a$ are the torques caused by drag forces due to the cable interaction with the fluid and $\vec{\tau}_e$ are torques due to the upthrust acting on each link. It is necessary to know the vectors of external forces as well as the

ISSN 2176-5480

vector position of the centers of mass of each link and also the center of mass of the end load are known, the torque are calculated from the vector product between the external forces and position of the points where the forces are acting on the cable.

Considering that the center of buoyancy of the links coincide with their respective center of mass, the buoyancy force has the same direction, but contrary to the gravitational force, which are equivalent to weights of the fluid volume because the links are submerged. Knowing the forces and their points of application, it is easy to obtain the torques due to these forces ($\vec{\tau}_e$). The drag forces were modeled as being proportional to the square of the speed between the cable and the fluid. The drag forces known provide the determination of torques due to drag represented by the vector $\vec{\tau}_a$.

5. SIMULATION RESULTS

Until the present time there is no an experimental setup to validate dynamic models. It is intended as a continuation of this research to build an experiment consisting of a cable equipped with several sensors to identify the parameters and validate the model. However, values have been assigned to the parameters of a dynamic model and simulations were performed, whose aim is to show that the proposed model provides consistent results with the expected dynamics for a cable submerged in water or not. A steel cable is employed with a diameter of 0.02*m* and length of 3.2*m,* with one end attached to a motionless body and the other free, with a mass of 0.5kg. For the simulations, it was considered $l_1=l_t/4$, $l_2=l_t/2$ and $l_3=l_t/4$, where l_t is the total length of the cable. This was a good choice that was found for the case of a model of a flexible link robot manipulator, as cited in reference [16]. However, it is still the subject of future research for the case of the dynamics of cables, ie, determining what is the best position to consider the fictitious joints. Probably, this can be clarified from the confrontation between experiments and simulations. The elastic constants, friction coefficients and the coefficients for the drag due to the contact with the fluid were assigned and refined in successive simulations to obtain physically expected results. The parameters used were as follows: k_{1e}=200; k_{2e}=200; k_{3e}=200 *Nm/rd* (joint fictitious elevation stiffness); k_{1a}=100; k_{2a}=100; k_{3a}=100 *Nm/rd* (joint fictitious azimut stiffness); k_{1t}=200; k_{2t}=200; k_{3t}=200 *Nm/rd* (joint fictitious azimut twist); c_{1e}=10.5; c_{2e}=0.5; c_{3e}=0.5 *Nms/rd* (elevation viscous friction coefficients); c_{1a}=4.2; c_{2a}=0.2; c_{3a}=0.2 *Nms/rd* (azimut viscous friction coefficients); c_{1t}=0.07; c_{2t}=0.035; c_{3t}=0.01 *Nms/rd* (twist viscous friction coefficients). When the cable is submerged in water, the drag forces were modeled simply as being proportional to the square of the relative velocity between the fluid and the cable. The drag coefficient was set $180Nms^2/rd^2$ and the forces are regarded as applied in the center of mass of each link.

The state vector of the dynamic system has nine coordinates of angular positions and nine other coordinates for the respective speeds. This means that three fictitious joints were considered. The simulations presented below were performed with the initial state formed with 0.1*rad* for each coordinate position and with all coordinate velocities set equal to zero. The external forces considered are the drag and the upthrust, existing when considering the underwater cable.

Fig. 5 shows the twist response, characterized by high frequencies and fast damping, as expected for cables whose material is steel. There are no significant changes in the twist response for cables out or underwater, because fluid dissipative effects due to the twist motion are negligible.

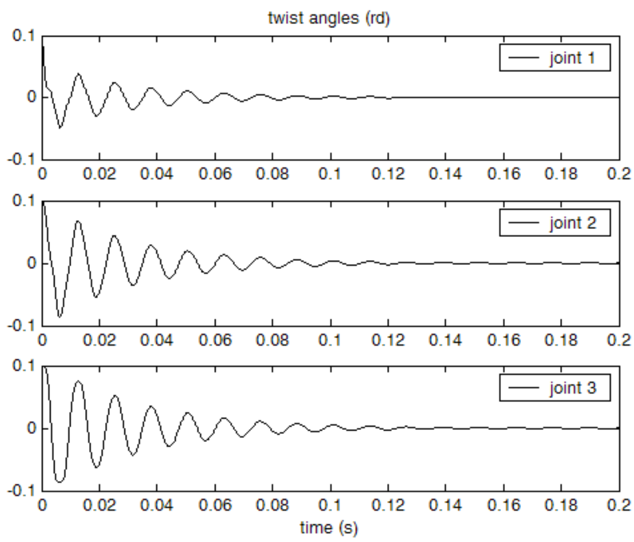

Fig. 5. Twist responses.

Fig. 6 shows the elevation and azimuth responses and also the spatial motion of the terminal load m_c . For the angular displacement, the graphics located at the top of the figure corresponds to the angular displacement of the first link; the intermediate graphs correspond to the second link, and the latest graphs to the third link. Note that the movement underwater is very damped, as expected because of the drag effects.

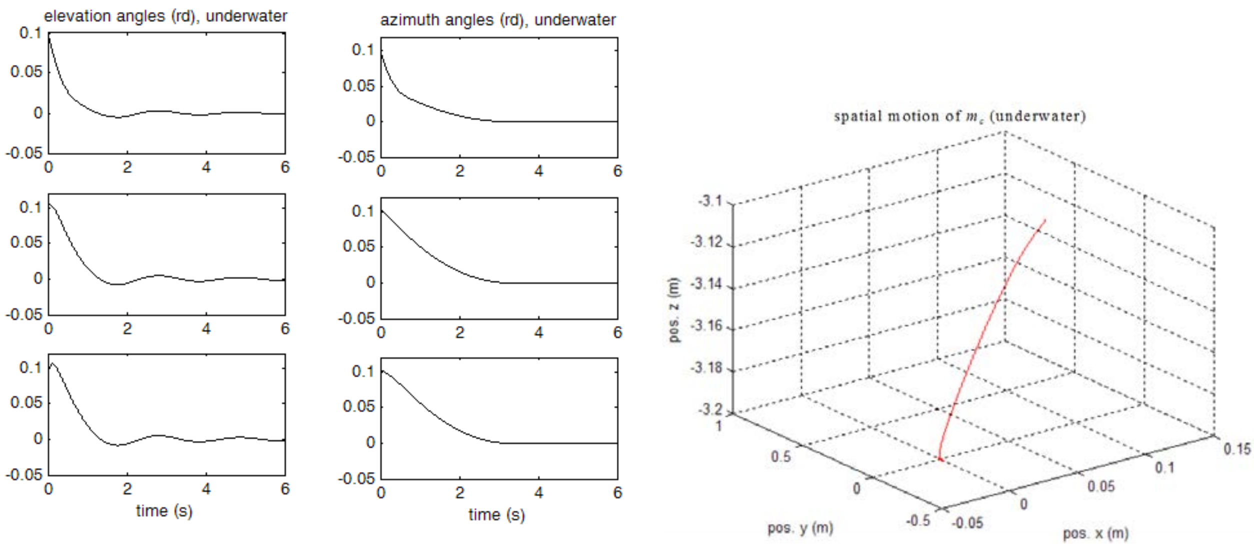

Fig. 6. Elevation and azimuth responses and spatial motion of m_c (Z coordinate was multiplied by -1).

6. CONCLUSIONS

This article investigated a new formalism for dynamic modeling of cables in underwater applications. The primary basis of the formulation is to assume that a continuous flexibility is represented by a discrete approach, consisting of rigid links connected by elastic joints, allowing the movement in the three-dimensional space. An important contribution of this proposition is the possibility of obtaining the Lagrangian of the system in an automatic way from a single equation, consisting of products and sums of terms that depend on the number of links considered, i. e., on the number of degrees of freedom to be adopted for the dynamic system. This equation to obtain the Lagrangian allows, for example, generating algorithms for the automatic determination of the dynamic model for any number of degrees of freedom. Values were adopted to the parameters of a dynamic cable model and simulations were performed, just to show that the model produce results consistent with the expected dynamic behavior of a cable underwater.
In the continuation of this research the authors pretend to develop an experimental support consisting of a cable and various sensors such as strain gauges and accelerometers to identify the model parameters and then to validate the work madding comparisons between numerical simulations and experiments. Another point is to determine the ideal length of the links. A study to clarify this point should be realized.

7. REFERENCES

[1] WANG, P.H., FUNG, R.F. and LEE, M.J. Finite Element analysis of a three-dimensional underwater cable with time-dependent length. Journal of Sound Vibration. Volume 209, Issue 2, January 1998, Pages 223-249.

[2] GOSLING, P.D. and KORBAN, F.A. A bendable finite element for the analysis of flexible cable structures. Finite Elements in Analysis and Design. 38 (2001) 45-63.

[3] ROCHINHA, A., SAMPAIO, R., and LE TALLEC, P. O Método do Lagrangeano Aumentado no Estudo de Cabos Umbilicais. Revista Internacional de Métodos Numéricos para Cálculo y Diseño em Ingenieria. Vol. 6,1, 97-108 (1990).

[4] SRINIL, N., REGA, G. and CHUCHEEPSAKUL,S. Two-to one resonant multi-modal dynamics of horizontal/inclined cables. Part I: Theoretical formulation and model validation. Nonlinear Dyn. (2007) 48:231-252.

[5] CORDOVÉS, D., Análise de Confiabilidade Estrutural de Cabos Umbilicais. Dissertação de Mestrado. Escola Politécnica da Universidade de São Paulo, 2008.

[6] YOON, J.W., PARK, T.W. e YIM, H.J. *Fatigue life prediction of a cable harness in an industrial robot using dynamic simulation.* Journal of mechanical science and technology. ISSN 1738-494X, 2008, Vol.22, nº 3, pp. 484-489.

[7] BUCKAM, B., DRISCOLL, F.R. and MEYER, N. *Development of a Finite Element Cable Model for Use in Low-Tension Dynamics Simulation.* J. Appl. Mech, July 2004-Volume 71,Issue 4, 476 (10 pages).

[8] MATULEA, I.C., et all. On the equilibrium configuration of mooring and towing cables. Applied Ocean Research, 30 (2008) 81-91.

[9] WANG, F., HUANG, G. and DENG, D. Steady State Analysis of Towed Marine Cables. J. Shanghai Jiaotong Univ. (Sci), 2008, 13(2):239-244.

[10] BLIEK, A. Dynamic analysis of single span cables. Cambridge, 1984. 295 f. Thesis (Doctor of Philosophy) – Departament of Ocean Engeneering, Massachusetts Institute of Technology).

[11] HOVER, F.S., GROSENBAUGH, M.A. and TRIANTAFYLLOU, M.S. Calculation of Dynamic Motions and Tensions in Towed Underwater Cables. IEEE Journal of Oceanic Engineering, Vol. 19, No. 3, July 1994.

[12] ZHU, K.-Q., ZHU, H.-Y., ZHANG,Y.-S. and GAO, J. *A multi-body space-coupled motion simulation for a deep-sea tethered remotely operated vehicle.* Journal of Hydrodinamic. 2008, 20(2):210-215.

[13] RAMAN-NAIR, W. and WILLIAMS, C.D. *Vortex-Induced Response of a Long Flexible Marine Riser in a Shear Current.* International Symposium on Technology of Ultra Deep Ocean Engineering. Feb 1-2, 2005, Tokyo, Japan.

[14] I. A. Bonev, C. M. Gousselin. Singularity loci of spherical parallel mechanisms. Proceedings of IEEE International Conference on Robotics and Automation. Barcelona, Spain, April, 2005.

[15] J. Breukels, W. J. Ockels. A multi-body dynamicos approach to a cable simulation for kities. IASTED Asian Conference on Modelling and Simulation, Beijing, China, Octuber, 2007.

[16] S. C. P. Gomes, V. S. Rosa and B. C. Albertini, "Active control to flexible manipulators," IEEE/ASME Trans. on Mechatronics, vol. 11, no. 1, pp. 75–83, USA, 2006.

[17] Pereira, A. E. L., Gomse, S. C. P. and Bortoli, A. L. A new formalism for dynamic modeling of cables. Mathematical Modeling and Computer Science, November, 2013.